Hindawi Publishing Corporation
International Journal of Photoenergy
Volume 2012, Article ID 154704, 6 pages
doi:10.1155/2012/154704

Research Article

Fabrication of Cu–Zn–Sn–S–O Thin Films by the Electrochemical Deposition Method and Application to Heterojunction Cells

Kai Yang and Masaya Ichimura

Department of Engineering Physics, Electronics and Mechanics, Nagoya Institute of Technology, Gokiso, Showa, Nagoya 466-8555, Japan

Correspondence should be addressed to Masaya Ichimura, ichimura.masaya@nitech.ac.jp

Received 16 April 2012; Accepted 13 July 2012

Academic Editor: Raghu N. Bhattacharya

A new multinary semiconductor $Cu_2ZnSnS_{4-x}O_x$ (CZTSO), which does not contain toxic elements and expensive rare metals, was fabricated by the electrochemical deposition (ECD) method. CZTSO thin films were deposited onto indium tin oxide (ITO-) coated glass substrates by DC and two-step pulsed ECD from aqueous solutions containing $CuSO_4$, $ZnSO_4$, $SnSO_4$, and $Na_2S_2O_3$. The films deposited by pulsed ECD contained smaller amount of oxygen than those deposited by DC ECD. The films had band gap energies in a range from 1.5 eV and 2.1 eV. By a photoelectrochemical measurement, it was confirmed that CZTSO films showed p-type conduction and photosensitivity. CZTSO/ZnO heterojunctions exhibited rectification properties in a current-voltage measurement.

1. Introduction

Recently, Cu_2ZnSnS_4 (CZTS) attracts much attention, as CZTS is suitable for thin film solar cells, owing to the bandgap energy of 1.4-1.5 eV and large absorption coefficient over 10^4 cm^{-1}. CZTS thin film solar cells were fabricated for the first time in 1988 by Ito and Nakazawa [1]. Efficiencies of up to 6.77% were achieved by Katagiri et al. [2]. Moreover, efficiency was further improved by adding Se into CZTS thin film. Several papers were reported on solar cells based on $Cu_2ZnSnS_{4-x}Se_x$ (CZTSSe), and Barkhouse et al. have fabricated 10.1% efficient CZTSSe cells by hydrazine-based solution processing [3]. Oxygen is another group VI element and can replace S in CZTS without disturbing valence. Therefore, $Cu_2ZnSnS_{4-x}O_x$ (CZTSO) can also be suitable for thin film solar cells. However, to our knowledge, there is only one paper on fabrication of CZTSO, which reports deposition of CZTSO by an open atmosphere type chemical vapor deposition using oxide precursors [4]. In this work, we deposit CZTSO thin films by the electrochemical deposition (ECD), which is a low-cost technique that enables the production of thin films in a large area in a short time.

ECD has been used to deposit metal precursors, which is subsequently sulfurized to form CZTS [5–7]. Recently, direct synthesis of CZTS by ECD has been reported [8–10]. However, in those previous papers, oxygen amount in the films was not mentioned at all, although introduction of some amount of oxygen is usually not avoidable in ECD from an aqueous solution. Thus, effects of oxygen on film properties have never been studied, and it has not been discussed either how the oxygen amount in a film can be controlled in ECD. Moreover, fabrication of heterostructure cells based on nonannealed ECD-CZTS has not been reported. In this work, we fabricate heterostructures based on as-deposited CZTSO films. So far, as a buffer layer, CdS was usually used for CZTS and CIGS-based solar cells [1–3, 11], but Cd is toxic and relatively rare. Recently, a Cd-free CZTS/ZnO heterojunction solar cell has been reported, and the conversion efficiency of 4.29% has been obtained [12]. Therefore, we selected ZnO as the partner of the pn heterojunction based on CZTSO.

2. Experimental

A three-electrode cell was used for ECD with a saturated calomel electrode (SCE) as the reference electrode.

Table 1: Deposition potential, composition, thickness, and bandgap of the CZTSO thin films.

Sample	Potential (V)	Cu (at %)	Zn (at %)	Sn (at %)	S (at %)	O (at %)	Thickness (μm)	Bandgap (eV)
A	V = −0.8	28.2	9.4	12.9	19.8	29.7	~0.5	2.1
B	V = −0.8~−0.5	28.4	11.3	8.8	30.9	20.6	~0.3	1.6
C	V = −0.9~−0.5	27.6	8.4	14.8	40.9	8.4	~0.3	1.6
D	V = −1.0~−0.5	22.6	16.3	13.0	28.8	19.2	~0.3	1.5
E	V = −1.1~−0.5	23.6	17.4	13.2	26.0	19.6	~0.3	1.6

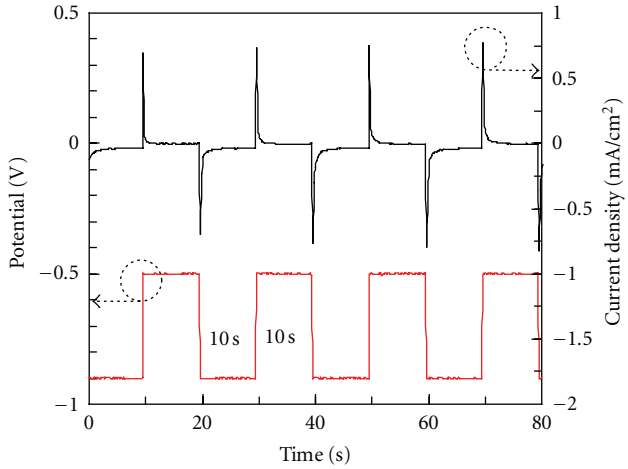

Figure 1: Two-step pulsed voltage and current profile during deposition of sample C.

Hokuto Denko function generator HB-104 and potentiostat/galvanostat HA-301 were used as the voltage source. Indium tin oxide (ITO-) coated glass was used as the working electrode (substrate), and a platinum sheet was used as the counter electrode. Both the ITO substrate and the platinum sheet were washed ultrasonically in alky benzene and dried in nitrogen before the experiment. The deposition area was about $1 \times 1\,\text{cm}^2$. The CZTSO thin films were prepared from an aqueous solution containing 5 mM $CuSO_4$, 5 mM $ZnSO_4$, 5 mM $SnSO_4$, and 25 mM $Na_2S_2O_3$, and 2 mL sodium lactate (59%) was added to 50 mL of the aqueous solution as a pH buffer [13, 14]. pH of the solution was 4.8. In a previous work, we succeeded in depositing Cu_xZn_yS using a similar solution containing lactate ions [15]. The electrolyte temperature was kept at room temperature in a water bath throughout the deposition. The deposition potential was determined on the basis of the cyclic voltammetry (CV). The cathodic scan was from 0 to −1.5 V, and the anodic scan was from −1.5 V to +0.5 V with a scan rate of 20 mV/s. Both DC and two-step pulse biases were employed for the deposition. The DC potential was determined to be −0.80 V on the basis of the cyclic voltammogram. The pulsed potentials employed for the deposition are listed in Table 1. The typical pulsed voltage and current profiles during deposition are shown in Figure 1. Total deposition time is 20 min. After the experiment, the deposited films were washed in pure water and naturally dried in air.

The compositional analyses were carried out by Auger electron spectroscopy (AES) using a JEOL JAMP 9500 Auger microprobe at a probe voltage of 10 kV and a current of 2×10^{-8} A. Argon ion etching with an acceleration voltage of 3 kV and a current of 8 mA was used to sputter the film surface. The surface morphology observation was also performed using scanning electron microscope (SEM) of JEOL JAMP 9500. The films thickness was measured by an Accretech Surfcom-1400D profile meter. The optical transmission measurement was performed using a JASCO U-570 spectrometer with the substrate as the reference. X-ray diffraction (XRD) was measured using a Rigaku Smartlab diffractometer with a Cu Kα radiation source.

To measure conduction type and photosensitivity, photoelectrochemical (PEC) measurements were carried out in an aqueous electrolyte containing 100 mM $Na_2S_2O_3$ using the same three-electrode cell as used for the deposition with the light incident from a xenon lamp toward the back side of the sample. The incident light was turned off and on mechanically every 5 s under the application of a ramp voltage.

ZnO was deposited by ECD using an aqueous solution containing 0.1 M $Zn(NO_3)_2$ [16]. The deposition temperature was 60°C. The deposition bias was a two-step pulse with $V_1 = -1.3$ V and $V_2 = -0.6$ V, and the duration of each pulse was 10 s. The deposition time was 2 min, and the film thickness was about 0.5 μm. Aluminum was evaporated as electrodes on the Al/CZTSO/ZnO/ITO glass substrate structure.

3. Results and Discussion

Figure 2 shows the AES spectra of samples A and C. The composition calculated from the AES results are listed in Table 1 and also plotted in Figure 3. The significant amount oxygen is included in the films. Introduction of oxygen is usually expected in ECD from aqueous solutions, and ECD of various oxides (ZnO [16, 17], SnO_2 [18, 19], Cu_2O [20, 21], and sulphide oxides (SnS_xO_y [22], ZnS_xO_y [23]) has also been reported. The source of oxygen in those oxide depositions is either OH^- ions or dissolved oxygen in the solution. In our case, since the solution is acidic (pH = 4.8), the dominant source of oxygen would be dissolved oxygen. The O/S ratio in the film is larger than unity for sample A, but it is smaller for the samples deposited by the pulsed potentials. Thus, the oxygen amount can be controlled by the deposition potential form. The previous works suggest that a slightly Zn-rich and Cu-poor

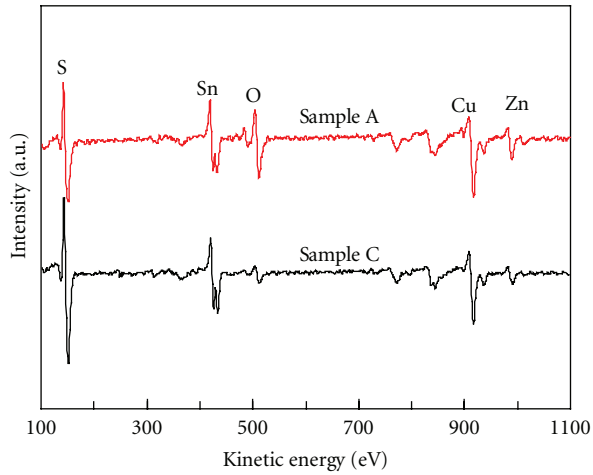

Figure 2: AES spectra for samples A and C.

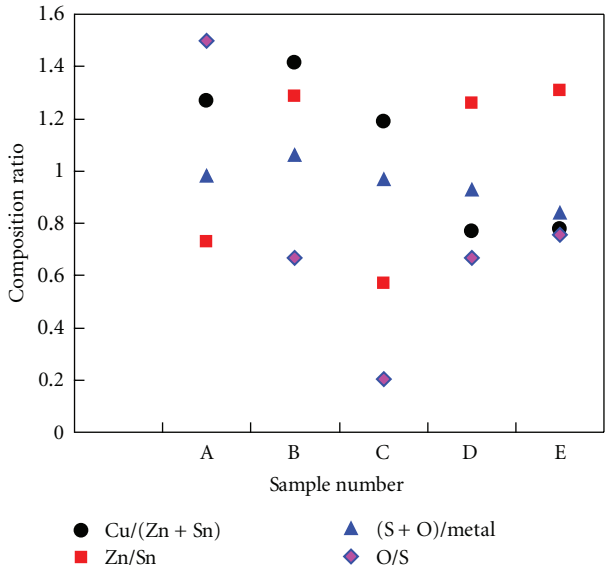

Figure 3: Composition ratios of the samples (A, B, C, D, and E).

composition gives good optoelectronic properties [24–26]. In case of the pulsed potential deposition, Cu amount was reduced with increasing negative potential, and samples D and E have Cu-poor composition (Cu/(Zn + Sn) < 1). This can be explained as follows. The ionization tendency is smaller (the equilibrium potential is more positive) for Cu than for Zn and Sn. Thus, deposition of the Cu-based compounds will start at more positive potential than the Zn and Sn-based compounds. Then the composition will be more Cu-rich at relatively positive deposition potentials. With increasing negative deposition potential, deposition rates of the Zn and Sn-compounds will be enhanced while deposition rate of the Cu-compounds is limited by supply of ions in the solution. Therefore, the composition is more Zn- and Sn-rich at a larger negative potential.

Figures 4(a) and 4(b) show the SEM images of samples A and D. For sample A, which was deposited by DC ECD, deposits with irregular shapes are seen on a continuous but porous film, whereas sample D seems to be composed of densely packed grains. The other samples deposited by pulsed ECD have surface morphology similar to sample D (Figure 4(b)). Thus, the films deposited by pulsed ECD are more dense than that deposited by DC ECD.

Figure 5 shows the optical transmission spectrum of samples A, B, C, D, and E. The films deposited by the pulsed potentials have an absorption edge at a longer wavelength than that deposited by DC ECD. Figure 6 shows plots of $(\alpha h\nu)^2$ versus $h\nu$, where α is the absorption coefficient and $h\nu$ the photon energy. In the calculation of absorption coefficient from the transmission data, a constant reflectance value (10%) was assumed, and the obtained bandgap values are listed in Table 1. The bandgaps of samples B–E are about 1.5–1.6 eV, close to the literature value of CZTS, while sample A has a bandgap larger than 2 eV. Since sample A is more oxygen-rich than the other samples, this indicates that the bandgap of CZTSO tends to increase with increasing oxygen content.

Figure 7 shows the PEC measurement results for the CZTSO films. The step-form variation in the current is due to the turning on/off of the illumination. By the illumination of the film, carriers are excited, and the excited minority carriers diffuse to the surface to participate in the electrochemical reaction at the film-electrolyte interface. Since the photocurrent is negative, the minority carriers generated here are electrons. Thus, we confirmed that the CZTSO films are p-type. The photocurrent is largest for sample D. This will be partly due to the fact that sample D has the smallest bandgap and thus can absorb largest number of photons among the samples. However, even if the number of absorbed photons is large, photoresponse will be small if recombination rate is high. Thus, the relatively large photocurrent for sample D implies that the defect density of sample D is comparable to or less than those of other samples. On the other hand, the optical transmission in the long-wavelength (subbandgap) region is lower for sample D than for the other samples, as can be seen from Figure 5. One might suppose that this low transmission is due to a large density of gap states, but then the photosensitivity would have been lower for sample D because of recombination at defect levels. Thus the low optical transmission of sample D could be due to some other reason, for example, scattering due to the grain structure.

Figure 8 shows the XRD patterns of the CZTSO films grown on ITO and the bare ITO substrate. For sample A, (112), (200), and (303) peaks of CZTS were confirmed in the XRD pattern, and Cu_2O (211) and Cu_4O_3 (303) peaks were also observed. It is considered that copper oxides were also formed because Cu/(Zn + Sn) > 1 and O/S > 1 for sample A. In the case sample B, C, D, and E, the major peaks of the film can be indexed as (112), (200), and (312) of CZTS. However, the peaks were very weak, probably because the films were not annealed or sulfurized and thus would be nanocrystalline or amorphous. The peaks of the copper oxides were not confirmed for samples B–E because oxygen amount was reduced to 20%–10% as can be seen from Table 1.

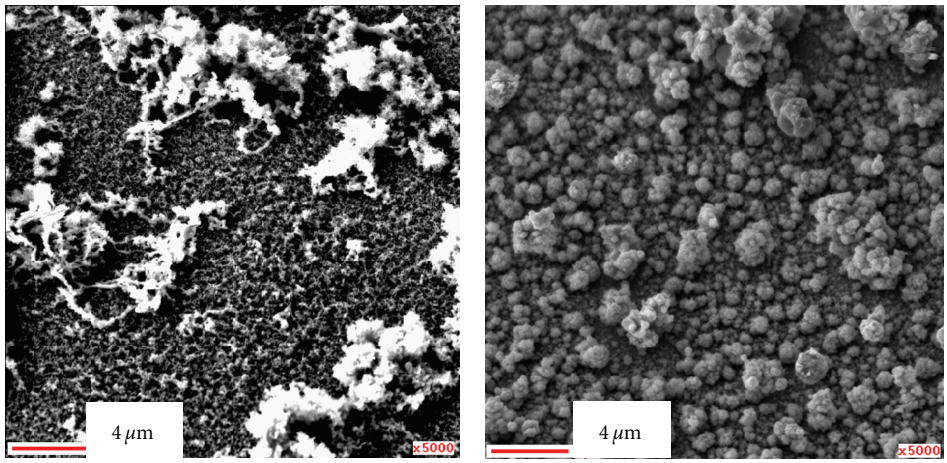

(a) (b)

Figure 4: SEM images of the surface of CZTSO (samples A and D).

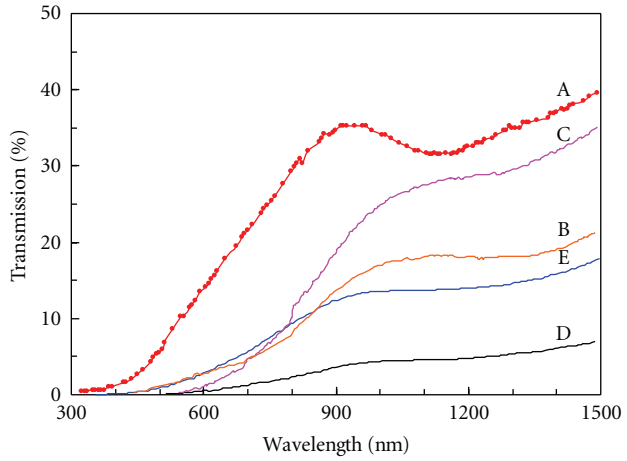

Figure 5: Optical transmission spectra of the CZTSO samples (A, B, C, D, and E).

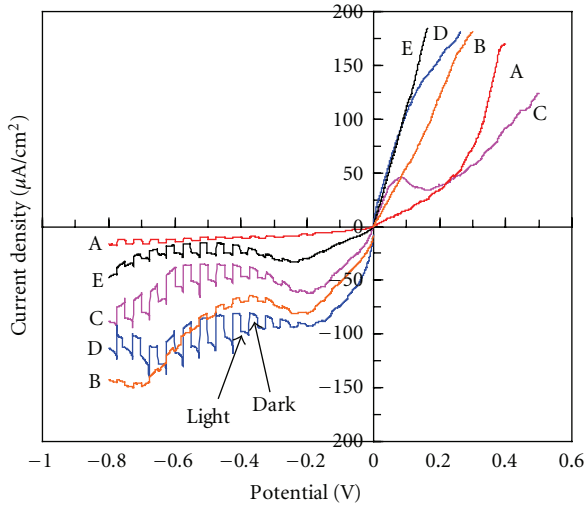

Figure 7: PEC measurement results of the CZTSO samples (A, B, C, D, and E).

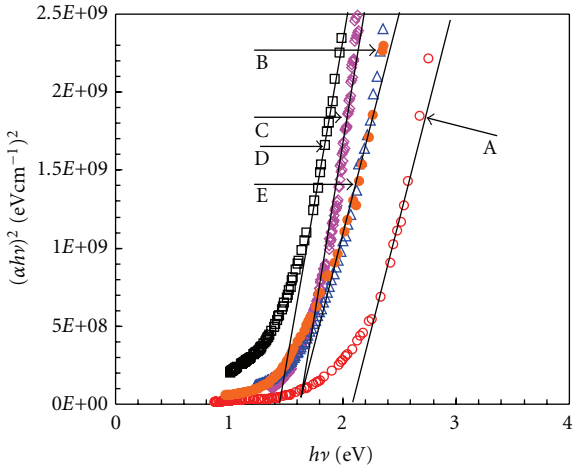

Figure 6: Estimation of the bandgap of the CZTSO samples (A, B, C, D, and E).

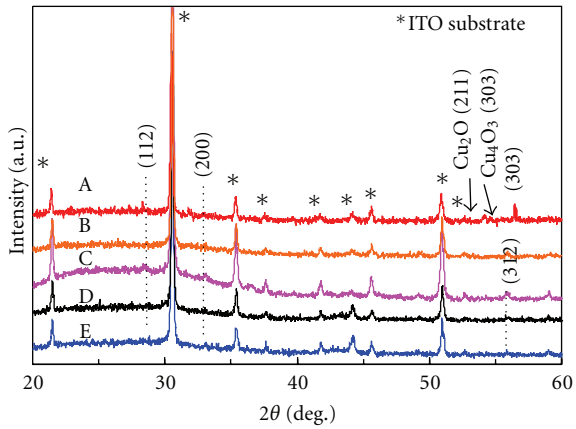

Figure 8: X-ray diffraction patterns of the CZTSO films (A, B, C, D, and E).

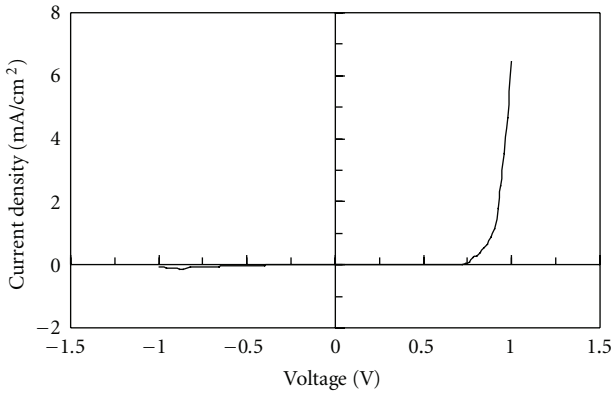

Figure 9: Current-voltage characteristics of the CZTSO/ZnO/ITO heterojunction cell (sample D).

Figure 9 shows the results of the current-voltage measurement in the dark for the heterostructure based on sample D. Rectification properties were observed, but the leakage current is large, about 0.15 mA/cm^2 at −1.0 V. The heterostructure based on the other CZTSO samples also shows similar rectifying behavior. However, the efficiency of those solar cells is very low probably because of the leakage current. Research is now in progress to improve efficiency by modifying the CZTSO deposition condition.

4. Conclusions

In this work, the DC and two-step pulsed ECD methods have been applied for fabricating CZTSO absorber layers for thin film solar cells. Oxygen amount in the film is smaller for the films deposited by pulsed ECD than that deposited by DC ECD, and composition is more Cu-poor for larger negative deposition potential. P-type conductivity and photosensitivity of the films are confirmed by the PEC measurement, and the pn heterojunction with ZnO shows rectification properties.

Acknowledgment

The authors would like to thank Dr. M. Kato for helpful discussion.

References

[1] K. Ito and T. Nakazawa, "Electrical and optical properties of stannite-type quaternary semiconductor thin films," *Japanese Journal of Applied Physics*, vol. 27, no. 11, pp. 2094–2097, 1988.

[2] H. Katagiri, K. Jimbo, S. Yamada et al., "Enhanced conversion efficiencies of Cu_2ZnSnS_4-based thin film solar cells by using preferential etching technique," *Applied Physics Express*, vol. 1, no. 4, Article ID 041201, 2 pages, 2008.

[3] D. A. R. Barkhouse, O. Gunawan, T. Gokmen, T. K. Todorov, and D. B. Mitzi, "Device characteristics of a 10.1% hydrazine-processed $Cu_2ZnSn(Se,S)_4$ solar cell," *Progress in Photovoltaics: Research and Applications*, vol. 20, no. 1, pp. 6–11, 2012.

[4] T. Washio, T. Shinji, S. Tajima et al., "6% Efficiency Cu_2ZnSnS_4-based thin film solar cells using oxide precursors by open atmosphere type CVD," *Journal of Materials Chemistry*, vol. 22, no. 9, pp. 4021–4024, 2012.

[5] H. Araki, Y. Kubo, K. Jimbo et al., "Preparation of Cu_2ZnSnS_4 thin films by sulfurization of co-electroplated Cu–Zn–Sn precursors," *Physica Status Solidi C*, vol. 6, no. 5, pp. 1266–1268, 2009.

[6] A. Ennaoui, M. Lux-Steiner, A. Weber et al., "Cu_2ZnSnS_4 thin film solar cells from electroplated precursors: novel low-cost perspective," *Thin Solid Films*, vol. 517, no. 7, pp. 2511–2514, 2009.

[7] J. J. Scragg, P. J. Dale, L. M. Peter, G. Zoppi, and I. Forbes, "New routes to sustainable photovoltaics: evaluation of Cu_2ZnSnS_4 as an alternative absorber material," *Physica Status Solidi B*, vol. 245, no. 9, pp. 1772–1778, 2008.

[8] M. Jeon, T. Shimizu, and S. Shingubara, "Cu_2ZnSnS_4 thin films and nanowires prepared by different single-step electrodeposition method in quaternary electrolyte," *Materials Letters*, vol. 65, no. 15-16, pp. 2364–2367, 2011.

[9] S. M. Pawar, B. S. Pawar, A. V. Moholkar et al., "Single step electrosynthesis of Cu_2ZnSnS_4 (CZTS) thin films for solar cell application," *Electrochimica Acta*, vol. 55, no. 12, pp. 4057–4061, 2010.

[10] Y. Cui, S. Zuo, J. Jiang, S. Yuan, and J. Chu, "Synthesis and characterization of co-electroplated Cu_2ZnSnS_4 thin films as potential photovoltaic material," *Solar Energy Materials and Solar Cells*, vol. 95, no. 8, pp. 2136–2140, 2011.

[11] M. A. Contreras, K. Ramanathan, J. Abushama et al., "Diode characteristics in state-of-the-art ZnO/CdS/$Cu(In_{1-x}Ga_x)Se_2$ solar cells," *Progress in Photovoltaics: Research and Applications*, vol. 13, no. 3, pp. 209–216, 2005.

[12] M. T. Htay, Y. Hashimoto, N. Momose et al., "A cadmium-free Cu_2ZnSnS_4/ZnO hetrojunction solar cell prepared by practicable processes," *Japanese Journal of Applied Physics*, vol. 50, no. 3, Article ID 032301, 4 pages, 2011.

[13] F. Kang, J. P. Ao, G. Z. Sun, Q. He, and Y. Sun, "Growth and characterization of $CuInSe_2$ thin films via one-step electrodeposition from a lactic acid/sodium lactate buffer system," *Materials Chemistry and Physics*, vol. 115, no. 2-3, pp. 516–520, 2009.

[14] F. Kang and M. Ichimura, "Pulsed electrodeposition of oxygen-free tin monosulfide thin films using lactic acid/sodium lactate buffered electrolytes," *Thin Solid Films*, vol. 519, no. 2, pp. 725–728, 2010.

[15] K. Yang and M. Ichimura, "Fabrication of transparent p-Type Cu_xZn_yS thin films by the electrochemical deposition method," *Japanese Journal of Applied Physics*, vol. 50, no. 4, Article ID 040202, 3 pages, 2011.

[16] M. Izaki and T. Omi, "Electrolyte optimization for cathodic growth of zinc oxide films," *Journal of the Electrochemical Society*, vol. 143, no. 3, pp. L53–L55, 1996.

[17] S. Peulon and D. Lincot, "Cathodic electrodeposition from aqueous solution of dense or open-structured zinc oxide films," *Advanced Materials*, vol. 8, no. 2, pp. 166–170, 1996.

[18] J. J. M. Vequizo, J. Wang, and M. Ichimura, "Electrodeposition of SnO_2 thin films from aqueous tin sulfate solutions," *Japanese Journal of Applied Physics*, vol. 49, no. 12, Article ID 125502, 5 pages, 2010.

[19] S. T. Chang, I. C. Leu, and M. H. Hon, "Preparation and characterization of nanostructured tin oxide films by electrochemical deposition," *Electrochemical and Solid-State Letters*, vol. 5, no. 8, pp. C71–C74, 2002.

[20] A. E. Rakhshani, A. A. Al-Jassar, and J. Varghese, "Electrodeposition and characterization of cuprous oxide," *Thin Solid Films*, vol. 148, no. 2, pp. 191–201, 1987.

[21] T. D. Golden, M. G. Shumsky, Y. Zhou, R. A. VanderWerf, R. A. van Leeuwen, and J. A. Switzer, "Electrochemical deposition of copper(I) oxide films," *Chemistry of Materials*, vol. 8, no. 10, pp. 2499–2504, 1996.

[22] K. Omoto, N. Fathy, and M. Ichimura, "Deposition of SnS_xO_y films by electrochemical deposition using three-step pulse and their characterization," *Japanese Journal of Applied Physics*, vol. 45, no. 3, pp. 1500–1505, 2006.

[23] N. Fathy and M. Ichimura, "Electrochemical deposition of $ZnO_{1-x}S_x$ thin films using three-step pulse," *Japanese Journal of Applied Physics*, vol. 44, no. 42–45, pp. L1295–L1297, 2005.

[24] T. Washio, H. Nozaki, T. Fukano et al., "Analysis of lattice site occupancy in kesterite structure of Cu_2ZnSnS_4 films using synchrotron radiation x-ray diffraction," *Applied Physics*, vol. 110, no. 7, Article ID 074511, 4 pages, 2011.

[25] H. Katagiri, K. Jimbo, W. S. Maw et al., "Development of CZTS-based thin film solar cells," *Thin Solid Films*, vol. 517, no. 7, pp. 2455–2460, 2009.

[26] Q. Guo, G. M. Ford, W. C. Yang et al., "Fabrication of 7.2% efficient CZTSSe solar cells using CZTS nanocrystals," *Journal of the American Chemical Society*, vol. 132, no. 49, pp. 17384–17386, 2010.